

RESEARCH

Open Access



Premature skeletal muscle aging in VPS13A deficiency relates to impaired autophagy

Veronica Riccardi¹, Carlo Fiore Viscomi², Marco Sandri^{2,3}, Angelo D'Alessandro⁴, Monika Dzieciatkowska⁴, Daniel Stephenson⁴, Enrica Federti¹, Andreas Hermann^{5,6,7}, Leonardo Salviati^{8,9}, Angela Siciliano^{1,10}, Immacolata Andolfo^{11,12}, Seth L. Alper¹³, Jacopo Ceolan^{1,10}, Achille Iolascon^{11,12}, Gaetano Vattemi^{10,14}, Adrian Danek¹⁵, Ruth H. Walker^{16,17}, Alexander Mensch¹⁸, Markus Otto¹⁸, Marcus Deschauer¹⁹, Moritz Armbrust^{20,21,22,23}, Cristiane Beninca²⁴, Valentina Salari¹, Paolo Fabene^{1,25}, Kevin Peikert^{5,6,7} and Lucia De Franceschi^{1,10*}

Abstract

VPS13A disease (chorea-acanthocytosis), is an ultra-rare autosomal recessive neurodegenerative disorder caused by mutations of the *VPS13A* gene encoding Vps13A. Increased serum levels of the muscle isoform of creatine kinase associated with often asymptomatic muscle pathology are among the poorly understood early clinical manifestations of VPS13A disease. Here, we carried out an integrated analysis of skeletal muscle from *Vps13a*^{-/-} mice and from VPS13A disease patient muscle biopsies. The absence of Vps13A impaired autophagy, resulting in pathologic metabolic remodeling characterized by cellular energy depletion, increased protein/lipid oxidation and a hyperactivated unfolded protein response. This was associated with defects in myofibril stability and the myofibrillar regulatory proteome, with accumulation of the myocyte senescence marker, NCAM1. In *Vps13a*^{-/-} mice, the impairment of autophagy was further supported by the lacking effect of starvation alone or in combination with colchicine on autophagy markers. As a proof of concept, we showed that rapamycin treatment rescued the accumulation of terminal phase autophagy markers LAMP1 and p62 as well as NCAM1, supporting a connection between impaired autophagy and accelerated aging in the absence of VPS13A. The premature senescence was also corroborated by local activation of pro-inflammatory NF-κB-related pathways in both *Vps13a*^{-/-} mice and patients with VPS13A disease. Our data link for the first time impaired autophagy and inflammaging with muscle dysfunction in the absence of VPS13A. The biological relevance of our mouse findings, supported by human muscle biopsy data, shed new light on the role of VPS13A in muscle homeostasis.

Keywords Autophagy, Energy, Inflammaging, Metabolome, NF-κB

*Correspondence:
Lucia De Franceschi
lucia.defranceschi@univr.it

Full list of author information is available at the end of the article



© The Author(s) 2025. **Open Access** This article is licensed under a Creative Commons Attribution-NonCommercial-NoDerivatives 4.0 International License, which permits any non-commercial use, sharing, distribution and reproduction in any medium or format, as long as you give appropriate credit to the original author(s) and the source, provide a link to the Creative Commons licence, and indicate if you modified the licensed material. You do not have permission under this licence to share adapted material derived from this article or parts of it. The images or other third party material in this article are included in the article's Creative Commons licence, unless indicated otherwise in a credit line to the material. If material is not included in the article's Creative Commons licence and your intended use is not permitted by statutory regulation or exceeds the permitted use, you will need to obtain permission directly from the copyright holder. To view a copy of this licence, visit <http://creativecommons.org/licenses/by-nc-nd/4.0/>.

Introduction

VPS13A disease or chorea-acanthocytosis is an ultra-rare autosomal recessive disorder affecting 1,000 patients worldwide with the onset of symptoms during young adulthood [52]. Chorea-acanthocytosis manifests as a progressive, usually choreic, movement disorder accompanied by behavioural and cognitive changes, epilepsy and peripheral neuropathy and/or myopathy [52]. Chorea-acanthocytosis is caused by mutations in the chromosome 9 gene *VPS13A* (vacuolar protein sorting 13 homolog A) encoding the protein VPS13A (or chorein), and thus was recently renamed “VPS13A disease” [70]. Although our understanding of VPS13A structure and function has progressed, much about its homeostatic roles in VPS13A disease target organs such as basal ganglia, the erythropoietic niche and skeletal muscle remain to be investigated. Studies of cellular and animal models of the disease suggest that absence of VPS13A results in altered vesicle trafficking, impaired autophagy and accumulation of autophagic markers [38, 62]. Of note, cellular models expressing VPS13A revealed that it mediates direct bulk lipid transfer between membranes (see [27] for review). We recently reported that *Vps13a*^{-/-} mice recapitulate hematologic and neurologic features of patients with VPS13A disease [53]. Of note, *Vps13a*^{-/-} mice show acanthocytes with retention of multivesicular body, dyserythropoiesis and signs of both hyper and hypokinetic movement disorders [53]. In isolated *Vps13a*^{-/-} basal ganglia we observed an impairment of autophagy involving the beclin-1 pathway, which was associated with accumulation of neurotoxic proteins such as active Lyn (phospho-Lyn), γ -synuclein and phospho-tau, suggesting dysfunctional proteostasis. Findings of neuroinflammation shown by *Vps13a*^{-/-} mice are shared with those of Parkinson’s disease (PD) and others among the more common neurodegenerative disorders [53].

The early onset increase of serum muscle phosphocreatine kinase (CK) in VPS13A disease has been linked to the heterogeneous neuromuscular manifestations of the disease, characterized mainly by peripheral neuropathy, but primary myopathic alterations can also be detected [52, 54, 67]. Clinically, neuromuscular involvement of VPS13A disease manifests very variably, ranging from asymptomatic hyper-CK-emia and areflexia to severe muscle atrophy and immobilizing paresis [54, 67]. In some cases, neuromuscular involvement may be one of the main factors affecting quality of life and independent living. Although VPS13A disease is often primarily referred to as a neurodegenerative disorder of the basal ganglia, it is clearly a multisystem disease also involving the neuromuscular system. However, the pathophysiology of muscular VPS13A deficiency and the heterogeneity of clinical involvement are still poorly understood. Currently, data on skeletal muscle involvement in

patients derive mainly from case series reporting (i) accumulation of tissue transglutaminase products, (ii) increase in number of small fibers associated with increased acid phosphatase activity; (iii) fascicular atrophy and (iv) selective fat infiltration [37, 44, 64, 67]. Although these reports describe patients with VPS13A disease at different disease stages, together they suggest a possible link between the VPS13A absence and autophagy perturbation in skeletal muscles from patients with VPS13A disease. The findings also resemble the reported acceleration of muscle aging by inhibition of autophagy [6, 8], characterized by increased oxidative damage and by accumulation of Neural Cell Adhesion Molecule (of NCAM) and other neuromuscular junction-enriched post-synaptic membrane components that are generally undetectable in adult myofibers. Of note, cytosolic and myolemmal relocalization of the accumulated NCAM is generally enriched near the neuromuscular junction, reflecting loss of myofiber innervation [6, 8].

Here, we bridge this gap by leveraging our recently described mouse model of VPS13A disease (*Vps13a*^{-/-} mice) [53]. Although the neurologic phenotype in mice manifests beyond the age of 12 months, we have focused our skeletal muscle analysis on early stage disease in 8 month-old *Vps13a*^{-/-} mice to minimize possible confounding effects of age [53]. *Vps13a*^{-/-} mice exhibited increased muscle damage and depleted energy stores, marked by impaired fatty acid oxidation, oxidative stress and disrupted autophagy pathways. Rapamycin treatment mitigated autophagy deficits and oxidative markers, highlighting the role of VPS13A deficiency in accelerating muscle aging, which is corroborated by observations in patient muscle biopsies.

Materials and methods

Mouse model and design of the study

Experiments were performed on age-matched WT (C57BL/6J) and *Vps13a*^{-/-} mice [53]. Since a gender effect on autophagy has been reported in models of neuromuscular disease such as Amyotrophic Lateral Sclerosis [19], we chose to study only female mice in the present study. WT and *Vps13a*^{-/-} mice underwent 24 h starvation as indicated. Both starved and fed mice were treated with either vehicle or colchicine (CLC) at the dosage of 0.4 mg/kg by intraperitoneal injection (i.p.) every 12 h for 3 times, as previously reported [63]. Two subgroups of *Vps13a*^{-/-} mice were treated with either vehicle or rapamycin (0.5 mg/Kg/d by i.p for 5 days) [35]. Isoflurane-anesthetized mice were randomly assigned to experimental groups and blindly analyzed [14]. Plasma creatine kinase (CK) was performed using standard biochemical assays [26]. Muscle wasting was evaluated as previously described [21]. Muscle MDA was determined as previously reported [39, 42]. We also studied muscle

biopsies from 3 patients with VPS13A disease compared to 3 control subjects without neuromuscular diseases (normal “myohistology”). Demographic data are shown in Table 1 S.

Behavioral test

A group of 26 (12 WT and 22 *Vps13*^{-/-}) female mice were tested on the Rotarod apparatus followed by CatWalk XT test the following day. Behavioral tests were performed on a consistent time window (09.00 a.m. – 01.00 p.m.) during the dark phase of the inverted 12/12-h light-dark cycle; mice were acclimated to the testing room for at least 30 min.

Rotarod

Mice were tested on the Rotarod apparatus (Ugo Basile, Varese, Italy). Before the test phase, animals underwent a training session consisting of three trials at a constant speed of 4 rpm for 3 min. Each session was separated by 30-minute inter-trial intervals. At the end of the training session, mice were returned to their home cage for 2 h. During the test phase, each animal underwent three trials (separated by 30-minute inter-trial intervals) at an accelerating speed from 4 to 40 rpm over 5 min. The mean latency to fall off the rotarod (average of the three trials) was used for statistical analysis. Pearson correlation analysis was used to assess the linear association between two continuous variables. The Pearson correlation coefficient (*r*) was employed as a quantitative measure of the strength and direction of the linear relationship between the variables.

CatWalk

Mice were tested on the CatWalk XT 10.7 (Noldus Information Technology BV, Wageningen, The Netherlands). The test consisted of three days of training to familiarize the mice to cross the walkway without hesitations, and a fourth day in which gait parameters were recorded (test day) [24]. On the test day gait parameters including run duration, run speed, swing speed, and stride length were evaluated in three runs without hesitation. All data analyses were performed with a pixel threshold value ≥ 25 arbitrary units.

Mouse histopathological analysis and electron microscopy

Histochemical and immunohistochemical analysis were carried out in skeletal muscles (tibialis and quadriceps) frozen in isopentane pre-cooled in liquid nitrogen and then sectioned at 8 μm in a cryostat. H&E, COX (cytochrome c oxidase), SDH (succinate dehydrogenase), acid phosphatase stains and p62 immunomicroscopy were performed by following standard protocols. Details are reported in Supplemental Materials.

Metabolomic analysis

Metabolomics analyses were performed as previously described [48]. Metabolites were extracted from snap-frozen muscle biopsies (10 mg) in 1 ml of ice-cold methanol/acetonitrile/water (5:3:2 v/v/v) [10], separated on a Kinetex XB-C18 column (Phenomenex), and analyzed using a UHPLC system (Vanquish, Thermo, San Jose, CA) coupled to a Q Exactive quadrupole-Orbitrap mass spectrometer (Thermo, San Jose, CA), as detailed by Nemkov et al. [48].

Immunoblot analysis

Immunoblot analysis was carried out on homogenized quadriceps as previously described [43, 53]. Details are reported in Supplemental materials.

RNA isolation, cDNA synthesis, and quantitative qRT-PCR

Quantitative RT-PCR (qRT-PCR) was performed by the SYBR-green method, following standard protocols with an Applied Biosystems ABI PRISM 7900HT Sequence Detection system. Details are reported in Supplemental materials.

Statistics

Two-tailed unpaired Student *t*-test or two-way analysis of variance with Tukey’s multiple comparisons were used for data analyses. Whenever indicated we used unpaired Student *t*-test or one-way ANOVA algorithm for repeated measures using Graph-pad 10.2. Normality was assessed with Shapiro-Wilk test. Data show values from individual mice and are presented as means \pm SEM. Differences with $p < 0.05$ were considered significant.

Results

Muscle biopsies from patients with VPS13A disease suggest a perturbation of autophagy also detected in skeletal muscle from *Vps13a*^{-/-} mice

Previous clinical case reports have suggested a possible link between the absence of VPS13A and perturbation of autophagy in the often mild or slowly progressive muscle symptoms of patients with VPS13A disease [29, 37, 44, 58, 64, 67]. We have therefore used our access to muscle biopsies from patients with VPS13A disease and healthy controls to further investigate this link. Patient clinical characteristics are reported in Table 1S. VPS13A was undetected in muscle biopsies from patients with VPS13A disease as compared with healthy controls (Fig. 1a). Patients with VPS13A disease exhibited increased muscle protein oxidation as determined by Oxyblot (Fig. 1b), associated with increased levels of the autophagy initiator LC3II (lipidated form of LC3) and with accumulation of the late phase autophagy markers LAMP1, LAMP2 and P62 (Fig. 1c, d). These data suggest the absence of VPS13A might sustain an impairment

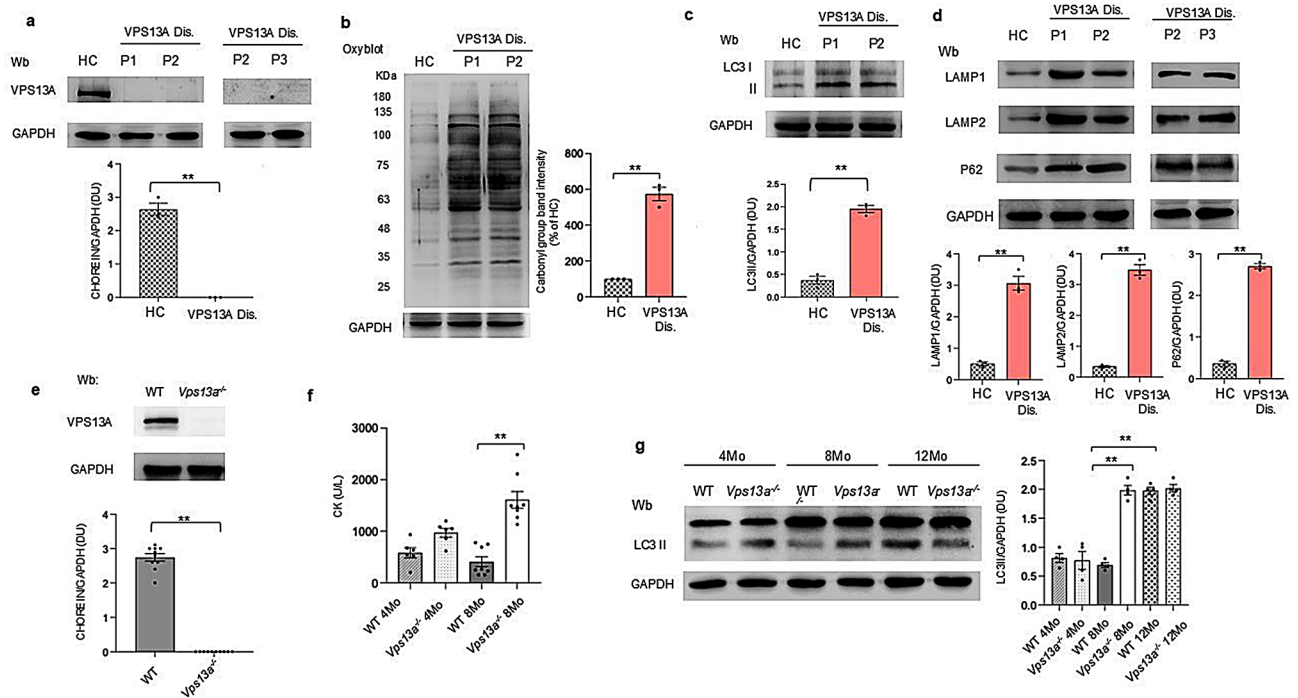


Fig. 1 Perturbation of autophagy is detectable in muscle biopsies from patients with VPS13A disease and in muscles from *Vps13a*^{-/-} mice. **(a)** Western-blot (Wb) analysis with specific antibody against Vps13A in muscle biopsies from patients with VPS13A disease (Dis.; P) and healthy controls (HC). GAPDH served as loading control. Below, densitometric analysis, means ± SEM (n = 3); **p < 0.002, paired Student t-test. **(b)** OxyBlot analysis of soluble fractions prepared from muscle biopsies of patients with VPS13A disease (Dis.; P) and controls. GAPDH, loading control. Representative of 3 similar experiments. Right, densitometric analysis, means ± SEM (n = 3); **p < 0.002, Student t-test. **(c)** Western-blot (Wb) analysis with specific antibody against LC3-I/II in muscle biopsies from patients with VPS13A disease (Dis.; P) and controls. GAPDH, loading control. Right, densitometric analysis, means ± SEM (n = 3); **p < 0.002, Student t-test. **(d)** Western-blot (Wb) analysis with specific antibodies against LAMP1, LAMP2 and P62 in muscle biopsies from patients with VPS13A disease (Dis.; P) and controls. GAPDH, loading control. Below, densitometric analyses, means ± SEM (n = 3); ***p < 0.002 by paired Student t-test. **(e)** Western-blot (Wb) analysis with specific antibody against Vps13A (VPS13A) in quadriceps lysate from wild type (WT) and *Vps13a*^{-/-} mice. GAPDH, loading control. Below, densitometric analysis, means ± SEM (n = 10); **p < 0.002 by unpaired Student's t test. **(f)** Plasma creatine kinase (CK) levels (U/L) in wild type (WT) and *Vps13a*^{-/-} mice aged 4 and 8 months (mo) (n = 6–10); *p < 0.05 by non-parametric Mann-Whitney test. **(g)** Western-blot (Wb) analysis with specific antibody against LC3-I/II in quadriceps lysate from WT and *Vps13a*^{-/-} female mice at ages 4, 8 and 12 mo. GAPDH, loading control. Right, densitometric analysis, means ± SEM (n = 4); *p < 0.002 by Mann-Whitney analysis.

of autophagy, favoring a pro-oxidant environment in patients with VPS13A disease. To better understand the role of VPS13A in muscle homeostasis, we studied *Vps13a*^{-/-} mice as a reliable model for VPS13A disease [53]. In *Vps13a*^{-/-} skeletal muscle, Vps13a expression was undetectable as compared to wild-type (WT) muscle (Fig. 1e), consistent with previous reports on skeletal muscle biopsies from patients with VPS13A disease [37, 44, 64, 67]. We found significant increase of plasma CK (Fig. 1f) and decreased muscle mass (Fig. 1Sa) in 8-month-old *Vps13a*^{-/-} mice compared to either 2-month-old *Vps13a*^{-/-} mice or WT animals. 8-month-old *Vps13a*^{-/-} mice exhibited a significantly worse performance on the Rotarod of *Vps13a*^{-/-} mice when compared to either WT controls or 2-months old *Vps13a*^{-/-} mice (Fig. 1Sb). Of note, worsening of performance of *Vps13a*^{-/-} mice was strictly correlated to muscle weight (Fig. 1Sc). To overcome possible limitation related to mouse weight, we used CatWalk gait analysis, focusing on parameters independent to body weight. The

gait analysis revealed significant alterations in locomotor parameters in *Vps13a*^{-/-} mice when compared to WT controls. Specifically, affected mice exhibited a prolonged run duration (Fig. 1Sd), and a significant reduction in run speed, stride length and swing speed (Fig. 1Se, f, g). These findings align with previous studies showing locomotor deficits in models of VPS13A disease and mirror the motor symptoms observed in human patients [53, 66]. In *Vps13a*^{-/-} mice (4–8 months of age), the muscle wasting was associated with significant increase of LC3-II when compared to matched WT animals, in agreement with human results (Fig. 1g). This difference was not found in 12-month-old mice, most likely related to age-dependent autophagy impairment as previously reported [6]. We therefore decided to focus further studies on 8 months old *Vps13a*^{-/-} mice.

Morphologic analysis of skeletal muscle by H&E stain and enzyme histochemical assessment of COX and SDH activity revealed no obvious alterations in *Vps13a*^{-/-} mice compared to WT animals (Fig. 2Sa). However, electron

microscopic (EM) examination revealed the presence of several autophagic structures, which were not detected in WT muscles (Fig. 2a). In addition, EM analysis of mitochondria showed increased mitochondrial area, reduced number of mitochondrial cristae and increased cristae width in *Vps13a*^{-/-} muscle compared to WT littermates, without change in length of cristae (Fig. 2b). These findings might reflect increased intracellular oxidation [30]. Accordingly, protein oxidation and lipid peroxidation in *Vps13a*^{-/-} skeletal muscle was higher than in WT muscle (Fig. 2c, d). These data together indicate that absence of VPS13a is associated with alteration of autophagy-lysosome system promoting muscle dysfunction. This conclusion was corroborated by the presence of muscle fibers with multiple small foci of acid phosphatase reactivity (red) in *Vps13a*^{-/-} muscle not-present in WT muscle (Fig. 2e).

Metabolomic analysis of skeletal muscles from *Vps13a*^{-/-} mice revealed severe energy stress and impaired fatty acid metabolism

As autophagy perturbation might affect muscle cell homeostasis and promote metabolic reprogramming [9, 22], we compared the metabolomes of *Vps13a*^{-/-} and

WT skeletal muscle. Mass spectrometry-based metabolomics revealed severe reduction in high energy phosphate compounds in *Vps13a*^{-/-} muscle (Fig. 3). Specifically, the observed depletion of ATP, ADP, GTP, GDP and UTP (lower half of the heat map in Fig. 3a and volcano plot in 3b) indicated severe impairment of energy metabolism, consistently reduced phosphocreatine pools. Reduced levels of NAD⁺ (Fig. 3a) and its nicotinate ribonucleotide precursor (Fig. 3a-b, and pathway analysis in 3c) were accompanied by accumulation of the NAD breakdown products ADP-ribose and nicotinamide (Fig. 3a and b), consistent with ADP-ribosyl cyclase-mediated catabolism of NAD [49]. Purine breakdown and oxidation products (allantoin) and salvage products (adenylosuccinate) accumulated in *Vps13a*^{-/-} mice (Fig. 3a and pathway analyses in panels c-d). Urea cycle activation (ornithine, argininosuccinate) and elevation in free amino acids (L-lysine, L-methionine, L-threonine, L-tryptophan) were consistent with defective amino acid metabolism, perhaps a consequence of increased turnover or decreased *de novo* protein synthesis (one of the most ATP-intensive of intracellular processes) [4]. Impaired fatty acid oxidation was noted, with accumulation of several acyl-carnitines in *Vps13a*^{-/-} muscle.

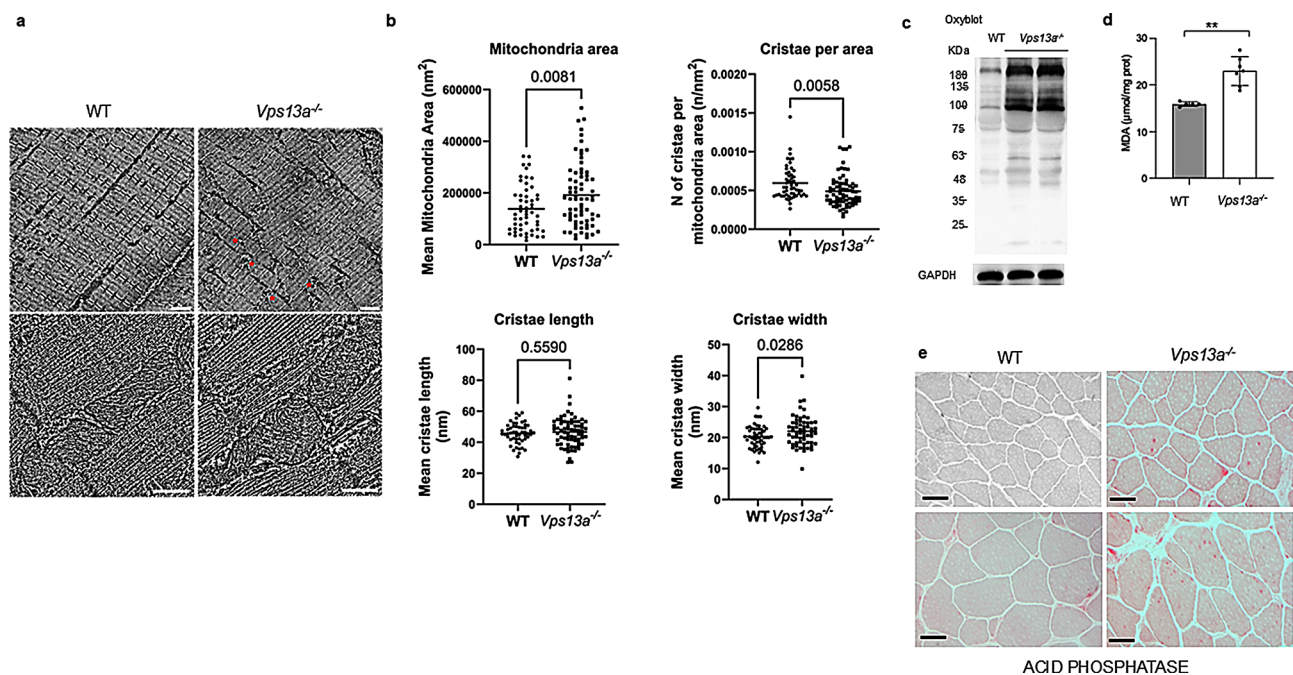


Fig. 2 *Vps13a*^{-/-} mouse skeletal muscle displays increased mitochondrial area with less but wider cristae, and signs of alteration autophagy-lysosome system associated with increased intracellular protein/ lipid oxidation. **(a)** EM analysis of WT (left) and *Vps13a*^{-/-} skeletal muscle (right). Upper panels: *Vps13a*^{-/-} muscle show the presence of altered myofiber structure and autophagic figures adjacent to mitochondria (asterisks), not detectable in WT muscles. Mitochondrial morphometry in WT and *Vps13a*^{-/-} 8-month-old quadriceps. Lower panels: higher magnification image highlighting mitochondrial ultrastructure. Scale bars: 2 μm for the upper panel, 200 nm for the lower panel. **(b)** Quantitative analysis of mitochondrial ultrastructure. Mitochondria show increased area and cristae number, but cristae appear wider. Unpaired Student's t tests. **(c)** OxyBlot analysis of quadriceps from 8-month-old WT and *Vps13a*^{-/-} female mice. GAPDH, loading control. Representative of 4 similar experiments. **(d)** Malondialdehyde (MDA) content of WT and *Vps13a*^{-/-} quadriceps. Means ± SEM (n=6), *p < 0.002 by unpaired Student's t test. **(e)** Acid phosphatase staining of skeletal muscle samples from WT (top) and *Vps13a*^{-/-} mice. In *Vps13a*^{-/-} mice a few muscle fibers show multiple small foci of acid phosphatase reactivity (appearing red). Scale bar is 40 μm.

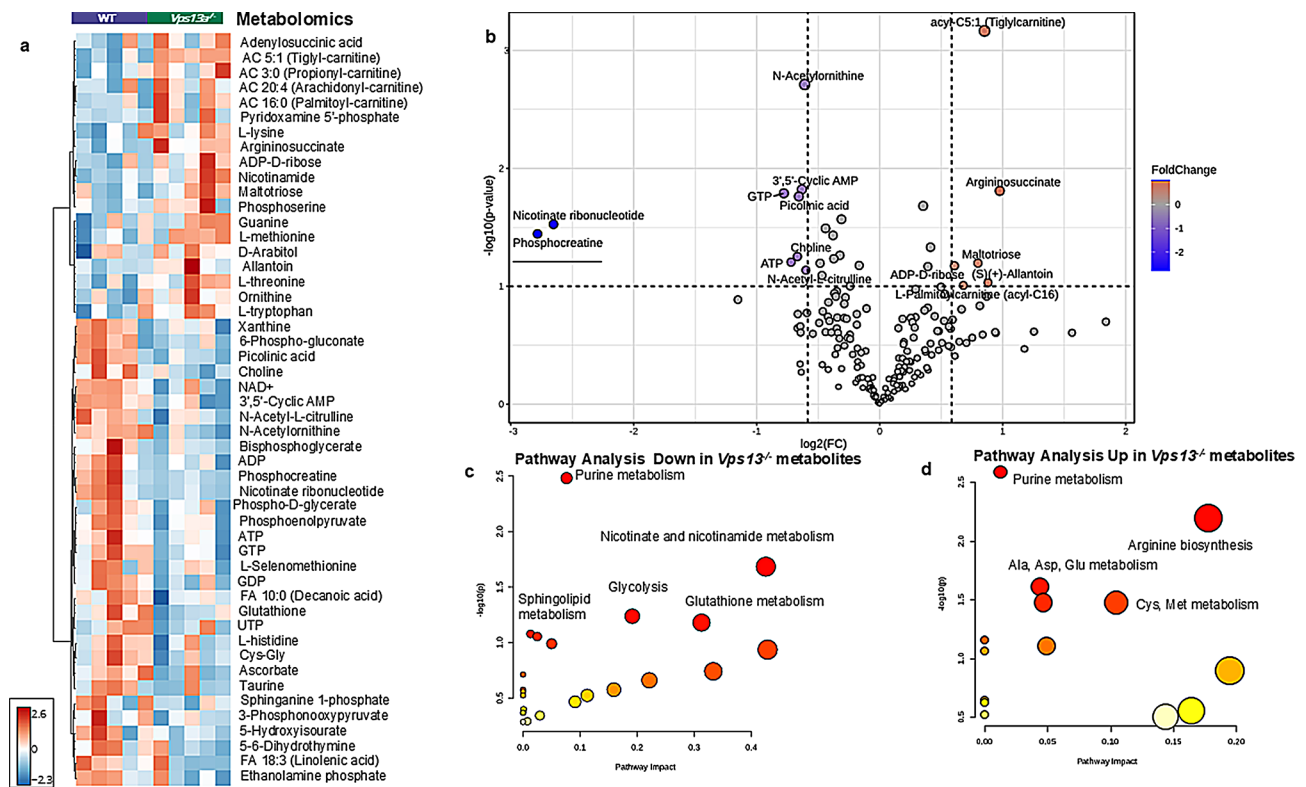


Fig. 3 *Vps13a^{-/-}* skeletal muscle metabolomics analysis highlights severe energy stress, impairment of fatty acid metabolism and depletion of phosphocreatinine pools consistent with muscle wasting. **(a)** Hierarchical clustering analysis of the top 50 metabolites by unpaired t-test. **(b)** Volcano plot of muscle metabolites elevated (red) or reduced (blue) in *Vps13a^{-/-}* vs. WT mice. Dotted axes mark thresholds of statistical significance or $\log_2(\text{FC})$. **(c)** **(d)** Pathway analysis of the most down-regulated (c) or up-regulated pathways (d) in *Vps13a^{-/-}* vs. control muscle.

Previous studies have shown that increased concentration of ACs is as marker of incomplete fatty acid oxidation to diagnose inborn fatty acid oxidation defects [40, 56]. More recently, incomplete fatty acid oxidation secondary to mitochondrial dysfunction has been recently shown in exercise intolerance in long COVID patients [25]. Of note, glycolytic precursors to ATP-synthesis steps, bisphosphoglycerate, phosphoglycerate and phosphoenolpyruvate were all depleted in *Vps13a^{-/-}* muscle. Increased oxidative stress in *Vps13a^{-/-}* muscle reflected not only increased purine deamination, but also depletion of the antioxidant ascorbate (vitamin C) and taurine. The combination of cell energy depletion, impaired fatty acid metabolism and increased oxidation might promote cell membrane weakness [15], favoring the CK release from muscle into the circulation, which characterized both mice and humans with VPS13A disease.

Proteomic analysis revealed defective autophagic responses and up-regulation of pro-apoptotic cascades

We next analyzed the proteomes of the same tissues to assess the abnormal proteostasis anticipated upon genetic ablation of *Vps13a*. Our results (Fig. 4) indicated down-regulation of metabolic enzymes (i.e. APRT for adenosine salvage/recycling– Fig. 4a). Volcano plot

analysis of the proteomics results revealed downregulation of PFKP (phosphofructokinase, platelet isoform), the rate limiting enzyme of glycolysis and a low abundance isoform (~11% in circulating blood cells other than platelets, less abundant than the muscle isoform), recently linked to bioenergetics in the context of severe ATP depletion [49]. Elevated levels of enzymes involved in iron metabolism and ferroptosis, such as STEAP3 [13], were associated with compensatory upregulation of VPS25 and other VPS proteins, and upregulation of protein damage-repair enzyme PCMT1. Pathway analysis of the top-most down-regulated and up-regulated processes in *Vps13a^{-/-}* mice identified impaired energetics, autophagy and elevated apoptotic cascades (Figs. 3c and 3Sb, c).

Increased protein oxidation in *Vps13a^{-/-}* muscle reflects a defective clearance of ubiquitinated components

The above findings prompted us to mine the proteomics results for post-translational modifications (PTMs). We first noted that proteins with PTM accumulated in *Vps13a^{-/-}* muscles (Fig. 5a). Ubiquitinated proteins, advanced glycation end-products (carboxyethyl-lysine) and irreversible cysteine oxidation (to dehydroalanine and, rarely, ammonia loss) were increased in *Vps13a^{-/-}* muscle (Fig. 5b-d), especially among mitochondrial

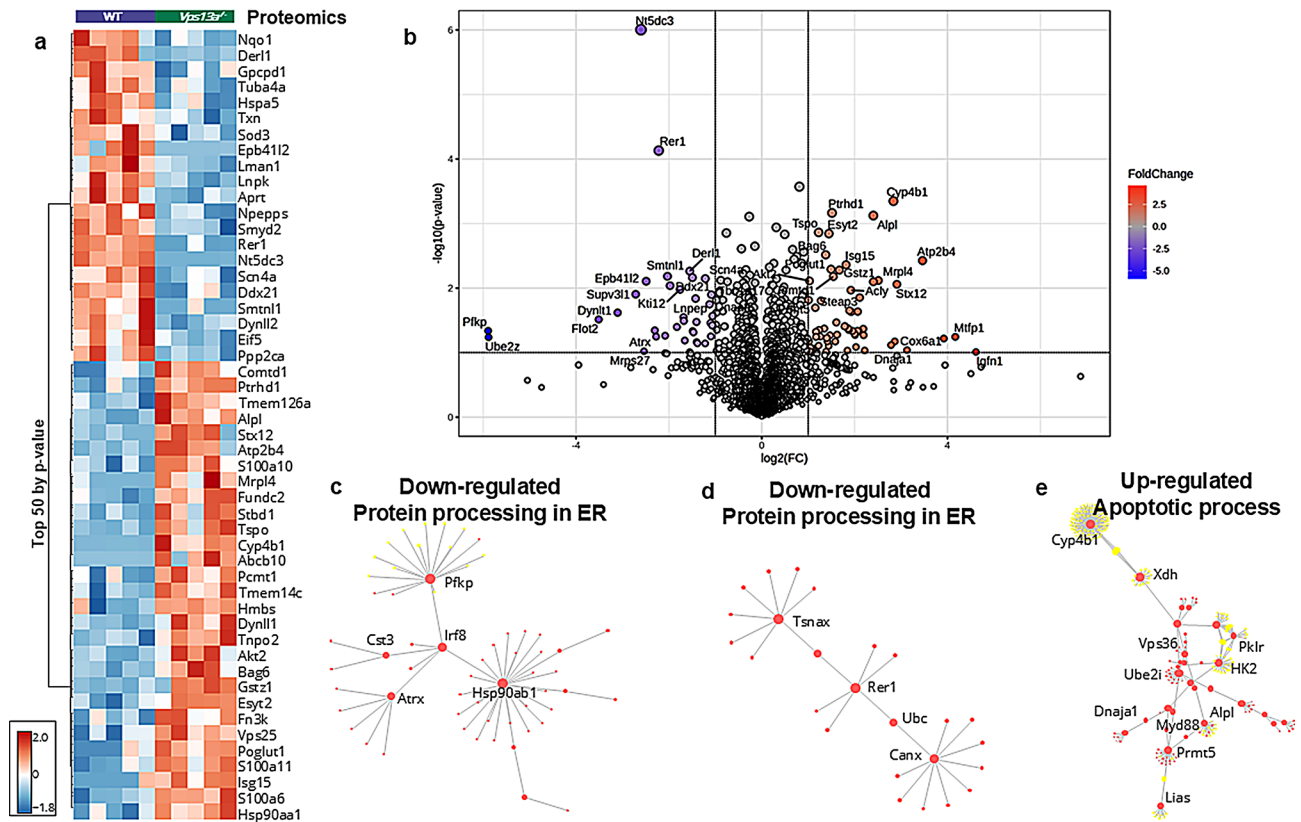


Fig. 4 *Vps13a*^{-/-} skeletal muscle metabolomics analyses suggest autophagy impairment leading to activation of pro-apoptotic pathways. **(a)** Hierarchical clustering analysis of the top 50 proteins by unpaired t-test. **(b)** Volcano plot of muscle proteins most downregulated (purple) or upregulated (red) in *Vps13a*^{-/-} vs. WT muscle. Dotted axes mark thresholds of statistical significance or log2(FC). **(c)** **(d)** **(e)** Pathway analysis of the most down-regulated pathways related to endoplasmic reticulum protein processing (c and d) and the most up-regulated pathways related to apoptotic processes (e) based on comparative proteomics of *Vps13a*^{-/-} and WT muscles.

electron transport chain complex components (NDUFS3, NDUV1, etc.), metabolic enzymes (ALDOA) and myofibril regulatory components (MYOM1, PYGM, RYR1, the last regulating calcium metabolism for myofibril contraction). The defective protein processing, down-regulated autophagic processes and up-regulated pro-apoptotic pathways in *Vps13a*^{-/-} muscle prompted our hypothesis that protein accumulation of PTMs, especially irreversibly modified moieties, may reflect, at least in part, defects in redox-sensitive and ATP-dependent proteolysis, through either ubiquitinyl-transferase or the proteasome. Indeed, ATP pool depletion in *Vps13a*^{-/-} mice was accompanied by elevations in ubiquitinated proteins, including several myosin light (MYLPE), and heavy chains (MYH4, MYH6, MYH7b), regulatory elements (RYR1) or ATP metabolic enzymes (adenylate kinase - AK, ATP13A5), cytochrome C (CYC) and glycolytic enzymes (ENO1). The metabolomics and proteomics data of *Vps13a*-deficient muscle together depicted a state of impaired energy metabolism, protein synthesis, autophagic responses and mitochondrial metabolism, accompanied by defects in myofibril stability and the myofibrillar regulatory proteome.

***Vps13a*^{-/-} muscle was characterized by impaired autophagy**

The broadly abnormal metabolomic profile of *Vps13a*^{-/-} muscle prompted further investigation of autophagy in *Vps13a*^{-/-} mice. We observed not only an elevated LC3II fraction (Fig. 1g), but in addition found overactivation of the autophagy initiator ULK1, as increased ULK1 phospho-form at Ser555 [16, 71] (Fig. 4Sa). These findings were associated with *Vps13a*^{-/-} muscle accumulation of VPS34 and ATG14, involved in the initial phase of autophagosome formation and of late phase autophagy-related proteins ATG5 and ATG7, RAB3, and lysosomal proteins LAMP1 and LAMP2 and P62 as compared to WT muscle (Figs. 6a, and 4Sb). Of note, in *Vps13a*^{-/-} mice displayed few muscle fibers with multiple small foci of P62 immunoreactivity, supporting the accumulation of P62 in the absence of VPS13A in skeletal muscle (Fig. 4Sc). Active Lyn also accumulated in *Vps13a*^{-/-} muscle to levels higher than in WT (Fig. 4Sd). These data taken together support a perturbation of autophagy-lysosome system in *Vps13a*^{-/-} muscle as compared to WT muscle. As proof-of-concept, we evaluated the effect of the known autophagy trigger, starvation, on

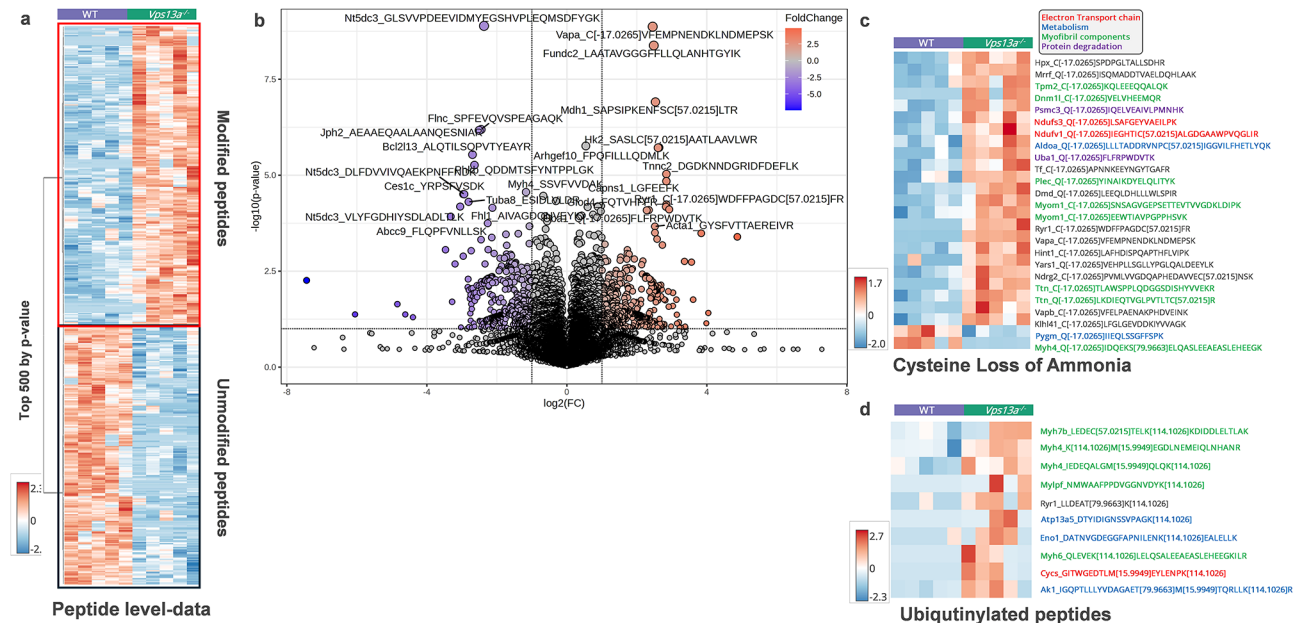


Fig. 5 Peptide-level analysis of *Vps13a*^{-/-} vs. WT muscles reveals increased oxidative modification and ubiquitination of proteins. **(a)** Heat map of the top 500 (unpaired t-test) peptide-level changes in *Vps13a*^{-/-} mice reveals increased levels of modified peptides and depletion of unmodified peptides. **(b)** Volcano plot of peptide level changes (red, higher in *Vps13a*^{-/-} mice; blue, lower in *Vps13a*^{-/-} mice). Dotted axes mark thresholds of statistical significance or log₂ (FC). **(c)** Cysteine modifications– including uncommon loss of ammonia– were increased in *Vps13a*^{-/-} mice. **(d)** Peptide level signatures of protein ubiquitination (K-GG) were increased in *Vps13a*^{-/-} mice, especially for myofibril light and heavy chain components.

muscles of both mouse strains. As expected, starvation should increase the autophagosome formation and consequently the LC3II lipidation without altering the lysosomal content [41, 46]. As shown in Fig. 6b, we found increased LC3II fraction without changing LAMP1 in muscle of starved as compared to fed WT mice. In contrast, muscle LC3II levels were indistinguishable in fed and starved *Vps13a*^{-/-} mice (Fig. 6b). This result was associated with LAMP1 accumulation in muscle from starved *Vps13a*^{-/-} mice in the absence of significant change in *Lamp1* gene expression when compared to starved WT animals (Fig. 5Sa). In order to test autophagy flux during the absence of nutrient, we blocked the autophagosome delivery to lysosome by CLC, causing the accumulation of autophagosome [32]. The autophagic flux results by the fold increase of LC3II band between treated and untreated mice. Figure 5Sb shows the combination of starvation and CLC increased LC3-II level in WT but not in *Vps13a*^{-/-} muscle. The combined data consistently support the conclusion that autophagy is impaired in muscles lacking VPS13A.

The muscle aging phenotype exacerbated by impaired autophagy can be rescued by Rapamycin

Previous studies have shown that the block of autophagy accelerates muscle senescence, contributing to neuromuscular junction (NMJ) instability. The resulting accumulation of neural cell adhesion molecule 1 (NCAM1) might be a marker of the skeletal muscle aging phenotype

[6, 8]. *Vps13a*^{-/-} muscle exhibited NCAM1 accumulation as compared to age-matched WT animals, supporting the hypothesis that impaired autophagy sustains protein oxidation to accelerate muscle aging (Fig. 6c). As a rescue experiment, we treated *Vps13a*^{-/-} mice with the autophagy activator, rapamycin [33, 35]. As shown in Fig. 6d, rapamycin markedly reduced accumulation of NCAM1 as well as of terminal phase autophagy markers LAMP1 and p62 (Fig. 6d). These data together support the hypothesis that absence of VPS13A exacerbates the aging phenotype of skeletal muscles through impairment of autophagy-lysosome system. The importance of our mouse data is supported by our observation of NCAM1 accumulation in muscle biopsies from patients with VPS13A disease (Fig. 6e).

Overactivation of the unfolded protein response system (UPR) in *Vps13a*^{-/-} mice further accelerates muscle aging

Activation of the UPR system in response to endoplasmic reticulum stress promoted by oxidation and accumulation of misfolded, damaged proteins is one of the hallmarks of skeletal muscle senescence [1, 36, 50]. The UPR is characterized by three branches driven by protein kinase R (PKR)-like endoplasmic reticulum kinase (PERK), inositol-requiring protein 1α (IRE1α), and activating transcription factor 6 (ATF6) [61]. Expression of ATF4, CHOP and GADD34 was higher in *Vps13a*^{-/-} than in WT muscle, whereas muscle ATF6 expression was indistinguishable in the two mouse strains (Figs. 7a, and

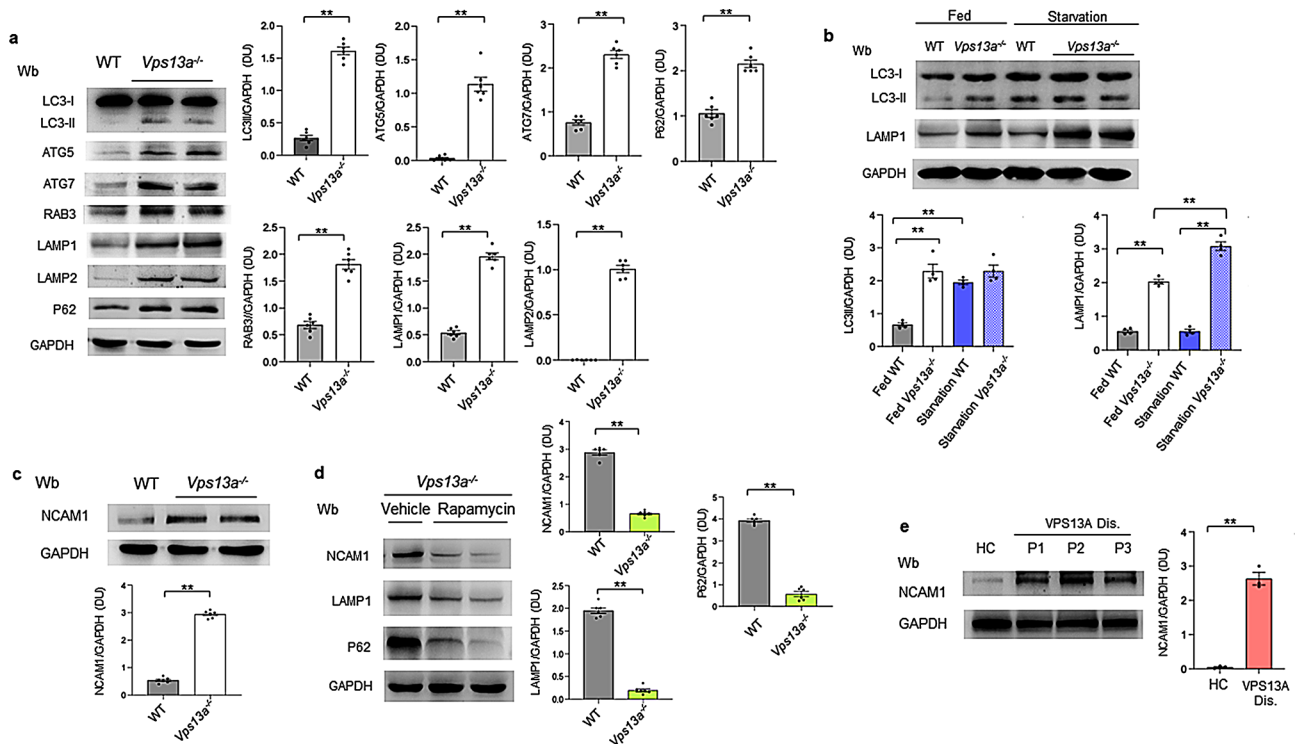


Fig. 6 The absence of Vps13A promotes impaired autophagy, exacerbating muscle aging phenotype. **(a)** Western-blot (Wb) analysis with specific antibodies against LC3-I/II, ATG5, ATG7, RAB3, LAMP1, LAMP2 and P62 in quadriceps lysates from *Vps13a*^{-/-} and WT female mice aged 8 months. GAPDH, loading control. Right, densitometric analysis. Means \pm SEM ($n=6$); $*p < 0.002$, unpaired Student t-test. **(b)** Western-blot (Wb) analysis with specific antibodies against LC3-I/II and LAMP1 in quadriceps lysates from *Vps13a*^{-/-} and WT female mice aged 8 months, *ad libitum* fed or starved for 24 h. GAPDH, loading control. Below, densitometric analyses. Means \pm SEM ($n=4$); $**p < 0.002$, paired Student-t-test. **(c)** Western-blot (Wb) analysis with specific antibody against NCAM1 in quadriceps lysates of *Vps13a*^{-/-} and WT female mice aged 8 months. GAPDH, loading control. Below, densitometric analysis. Means \pm SEM ($n=6$); $**p < 0.002$, unpaired Student t-test. **(d)** Western-blot (Wb) analysis with specific antibodies against NCAM1, LAMP-1 and P62 in quadriceps lysates of 8-month-old *Vps13a*^{-/-} or WT female mice treated with rapamycin (2 mg/kg, intraperitoneally injected every 24 h for 5 days). GAPDH, loading control. Right, densitometric analyses. Means \pm SEM ($n=6$); $**p < 0.002$, unpaired t-test. **(e)** Western-blot (Wb) analysis with anti-NCAM1 antibody of lysates from muscle biopsies of patients with VPS13A disease (Dis.; P) and control. GAPDH, loading control. Right, densitometric analysis. Means \pm SEM ($n=3$); $*p < 0.002$, paired Student t-test.

6Sa). As expected, starvation increased expression of ATF4 and CHOP in WT but not in *Vps13a*^{-/-} muscle. CHOP might be considered a pro-apoptotic factor common to the three branches of the UPR system, and prolonged CHOP expression might up-regulate expression of GADD34, another pro-apoptotic mechanism driving cells towards caspase activation [1, 36, 50]. Increased expression of both CHOP and GADD34 in *Vps13a*^{-/-} muscle resulted in caspase 3 activation and increased caspase 8 expression as compared to WT muscle, associated with activation of the cell death pathway initiator p53 (Figs. 7a and 6Sb, c). Thus, *Vps13a*^{-/-} skeletal muscle was characterized by a pro-apoptotic molecular signature sustained by impaired autophagy, UPR overactivation and pathologic metabolic reprogramming.

Inflammaging contributes to premature aging of *Vps13a*-deficient skeletal muscle

Previous studies have shown that muscle aging is associated with the local activation of pro-inflammatory and

redox response transcriptional factors such as NF- κ B and Nrf2 [2, 23, 57, 60, 68, 69]. As shown in Fig. 7c, we detected age-dependent activation of both NF- κ B and Nrf2 in *Vps13a*^{-/-} muscle as compared to WT muscle. NF- κ B activation was higher in 12-month-old than in 2-month-old WT muscle (Figs. 7c and 7S), highlighting the potential role of NF- κ B activation in inflammaging of muscle from *Vps13a*^{-/-} mice. Indeed, *Vps13a*^{-/-} muscle genes up-regulated at 8 months of age included the NF- κ B-regulated pro-inflammatory cytokines *Il-6*, *TNFA*, *Il-1b* (Fig. 7d). Peak Nrf2 activation was found in *Vps13a*^{-/-} muscle at 8 months of age when severe energy stress and protein oxidation were detected (Fig. 7c and 7S). Consistently, the expression of Nrf2-regulated *Nqo1* and *Ho-1* antioxidant systems were also induced (Fig. 7d). Of note, up-regulated muscle expression of IL-1 β and other pro-inflammatory cytokines has been reported in a mouse model of Parkinson disease (PD), and is part of the senescence-associated phenotype contributing to PD sarcopenia [17, 51, 55]. In muscle biopsies from patients

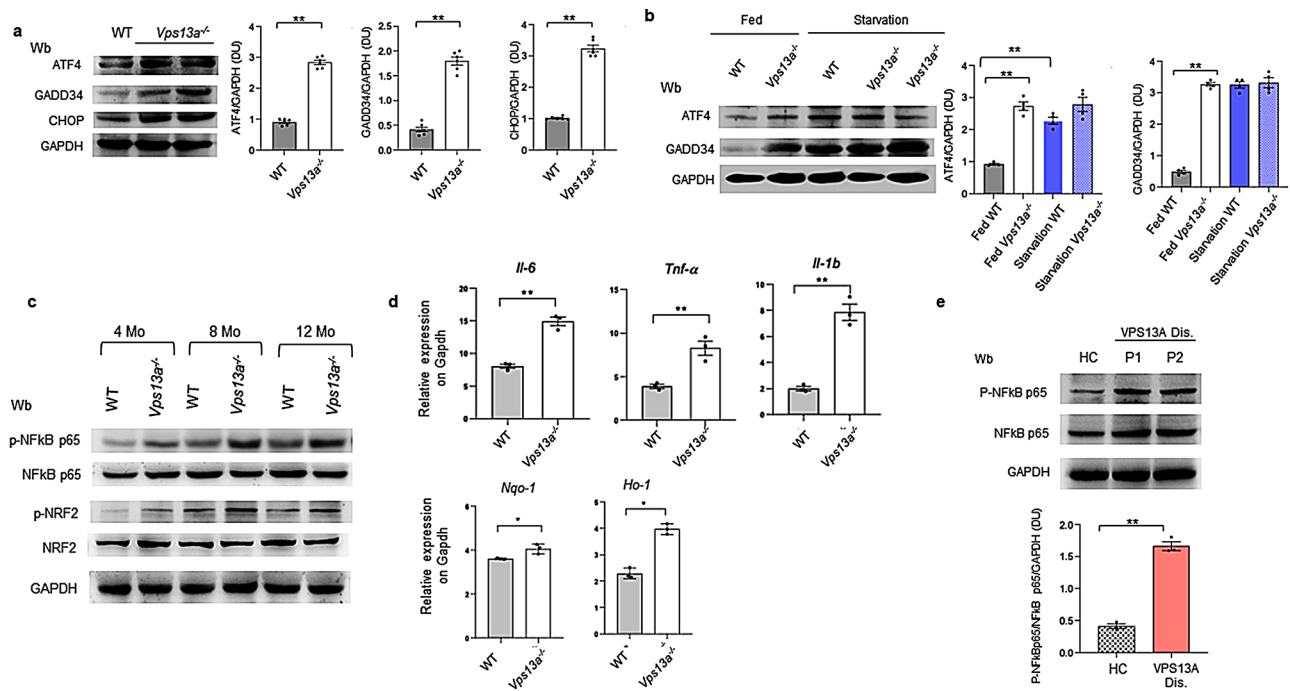


Fig. 7 Skeletal muscles lacking Vps13A display overactivation of UPR and sustained local inflammatory response, supporting a contribution of inflammation in muscle dysfunction of VPS13A disease. **(a)** Western-blot (Wb) analysis with specific antibodies against ATF4, GADD34 and CHOP in quadriceps lysates from WT and *Vps13a*^{-/-} female mice aged 8 months. GAPDH, loading control. Right, densitometric analyses. Means ± SEM (n=6); * p < 0.05, ** p < 0.002, one-way ANOVA. **(b)** Western-blot (Wb) analysis with specific antibodies against ATF4 and GADD34 in quadriceps lysates from 8-month-old wild type (WT) and *Vps13a*^{-/-} female *ad libitum* fed or starved for 24 h. GAPDH, loading control. Right, densitometric analyses. Means ± SEM (n=6); * p < 0.05, paired Student t-test. **(c)** Western-blot (Wb) analysis with specific antibodies against phospho-NF-kB (Ser536), NF-kB, phospho-NRF2 (Ser40) and NRF2 in quadriceps lysates of WT and *Vps13a*^{-/-} female mice at 4, 8 or 12 months of age. GAPDH, loading control (see Fig. 4E.V for densitometric analysis). **(d)** Quadriceps RNA levels of *Il-6*, *Il-1β*, *Tnf-α*, *Nqo-1* and *Ho-1* normalized to *Gapdh* RNA in WT and *Vps13a*^{-/-} mice aged 8 months. Means ± SD (n=3) (** p < 0.01, ANOVA test and post-hoc correction by Tukey's multiple comparison tests). **(e)** Western-blot (Wb) analyses with specific antibodies against p-NF-kB (Ser536) and NF-kB in muscle biopsies from with VPS13A disease (Dis.; P) and controls. GAPDH, loading control. Below, densitometric analysis. Means ± SEM (n=3); ** p < 0.002, paired Student t-test.

with VPS13A disease, we found activation of NF-kB as compared to healthy controls (Fig. 7e). Collectively, our data corroborates the working hypothesis that impaired autophagy in the absence of VPS13A is associated with a premature muscle aging phenotype.

Discussion

Here, we show for the first time that the absence of Vps13a in skeletal muscle impairs autophagy and secondarily promotes metabolic reprogramming similar to that of aging and other conditions [8]. The metabolome of *Vps13a*^{-/-} skeletal muscle revealed severe depletion not only of phosphocreatine pools, but also of all high energy phosphate reservoirs. Altered adenylate pools could be explained in part by defective glycolysis, as evidenced by irreversible post-translational modifications to ALDOA and ENO1 and by severe depletion of PFKF, a PFK isoform upregulated when normal ATP levels fall >80%. ATP depletion was likely exacerbated further by increased ubiquitination of AK, normally rate-limiting for adenylate pool preservation in the face of energetic challenge. Additional contributors to altered

adenylate pools included dysregulated fatty acid metabolism as reflected in accumulation of acyl-carnitines. Purine breakdown and deamination was accompanied by depletion of NAD⁺ (and of its precursor nicotinate ribonucleotide) with elevation of its breakdown products ADP-ribose and nicotinamide, consistent with activation of ADP-ribosyl cyclases 1 and/or 2 (CD38/BST1) [49]. Of note, NAD pool reduction is a hallmark of aging and sarcopenia [11, 45] and oral NAD precursor supplementation has been proposed as a strategy to delay onset of age-related comorbidities [3].

Defects in autophagic cascades were incompletely compensated either by ATP-dependent proteasomal degradation of existing protein components or by *de novo* protein synthesis, arguably (along with ionic homeostasis) the most ATP-intensive of cellular processes. In this context, ER Ca²⁺ release channel and contractility regulator RYR1 of Vps13a-deficient muscle was irreversibly oxidized at cysteine residues and hyper-ubiquitinated, as compared to WT muscle. Accumulation of ubiquitinated myofibrillar light and heavy chain components, along with increased expression of protein damage repair

enzymes such as the isoaspartate modifier L-isoaspartyl O-methyl transferase [12] was accompanied by increased levels of the ferrireductase STEAP3 [13] and other promoters of ferroptosis. The metabolic and proteomic profiles of *Vps13a*^{-/-} muscle further support impairment of autophagy as a contributor to muscle dysfunction in (i) the lack of skeletal muscle autophagy activation in response to starvation and to starvation *plus* colchicine treatment; and (ii) the rescue of skeletal muscle autophagy in rapamycin-treated *Vps13a*^{-/-} mice.

The impairment of autophagy in *Vps13a*^{-/-} muscle resembled aspects of accelerated aging. Indeed, *Vps13a*^{-/-} muscle exhibited accumulations of oxidized contractile proteins and NCAM1, both markers of early skeletal muscle senescence [6]. This observation was further corroborated by NCAM1 accumulation observed in muscle biopsies from patients with VPS13A disease, which suggests an instability of muscle nerve synapse. Overactivation of UPR (likely in response to sustained ER stress) served as additional evidence of premature muscle cell senescence in the absence of VPS13A. The insensitivity to starvation of ATF4 and GADD34 levels in *Vps13a*^{-/-} skeletal muscle suggested UPR saturation, contributing to a pro-apoptotic profile including increased activities of caspase-3 and -8, and elevations in the ancillary senescence marker phospho-p53, in agreement with our proteomic data [7, 72]. Under physiologic condition, activation of UPR system by taking care of both protein folding and degradation within ER, contributes to skeletal muscle cell homeostasis. However, persistent overactivation of the UPR system results in accumulation of unfolded, oxidized proteins, contributing to cell muscle dysfunction. Whenever overactivation of UPR is combined with impaired autophagy, cells are redirected towards pro-apoptotic pathways, ending in muscle waste and sarcopenia [18, 31]. In addition, sustained ER stress and overactivation of the UPR system can trigger a pro-inflammatory signaling through the activation of an NF- κ B response [28, 34]. Indeed, *Vps13a*^{-/-} mice display skeletal muscle activation of redox and inflammation-related transcriptional factors NF κ B and NRF2, with up-regulation of their downstream gene targets such as *Il-1b* and *Nqo1*. Previous studies have shown that sterile inflammatory status activating NF- κ B pro-inflammatory pathways generates a premature senescent environment (inflammaging theory) [20, 59]. This might contribute to age related muscle waste and sarcopenia [5, 65]. The activation of NRF2 pathway might try to cope chronic cell oxidation, to limit cell damage and ensure cell survival [47]. Collectively our data support a premature cell muscle aging in the absence of VPS13A. The clinical relevance of our novel findings in *Vps13a*^{-/-} mice is supported by muscle biopsies from patients with VPS13A disease, which exhibit a premature aging

phenotype, again characterized by (i) impaired autophagy with increased protein oxidation; (ii) accumulation of NCAM1; and (ii) chronic activation of NF- κ B. Our data may contribute to clinical management of patients with VPS13A disease, suggesting a possible benefit of early exercise intervention to delay the muscle wasting that is expected to accelerate in response to subsequent/additional peripheral neuropathy.

Study limitations

Our study has two major limitations. First, the study focused on 8-month-old *Vps13a*^{-/-} mice, younger in age than the 12–14-month-old mice with abnormal behavioral test results in our previous study [53]. As skeletal muscle activation of autophagy and NF κ B was evident in 12-month-old WT mice, we chose 8 months of age as an optimal experimental time to avoid possible confounding effects of physiologic aging. However, histopathologic analysis of older mice might be considered for future study. Second, as VPS13A disease is an ultrarare disease, the number of muscle biopsies available for this study was limited.

Conclusions

Our data shed new light on the mechanism of muscle dysfunction in VPS13A disease. We show for the first time that absence of VPS13A results in impaired autophagy in skeletal muscle, which markedly alters the metabolic profile. Cellular energy depletion combined with prolonged protein oxidation leads to inflammaging and muscle dysfunction in patients with VPS13A disease. Future studies in a larger cohort of patients with VPS13A disease may further confirm the link between impaired autophagy and the accelerated aging phenotype in the absence of VPS13A.

Abbreviations

VPS13A	Vacuolar protein sorting 13 homolog A
NCAM1	Neural Cell Adhesion Molecule
CLC	Colchicine
CK	Creatine Kinase
MDA	Malondialdehyde
H&E	Hematoxylin & Eosin
COX	Cytochrome c oxidase
SDH	Succinate dehydrogenase
LC3	Microtubule-associated protein 1 A/1B-light chain 3
LAMP1	Lysosomal associated membrane protein 1
LAMP2	Lysosomal associated membrane protein 2
p62	Sequestosome-1
ATP	Adenosine triphosphate
ADP	Adenosine diphosphate
GTP	Guanosine triphosphate
GDP	Guanosine diphosphate
UTP	Uridine triphosphate
NAD	Nicotinamide adenine dinucleotide
APRT	Adenine phosphoribosyltransferase
PFKP	Phosphofructokinase
VPS25	Vacuolar protein sorting 25
PCMT1	Protein-L-isoaspartate O-methyltransferase
PTM	Post-translational modifications

NDUFS3	NADH dehydrogenase [ubiquinone] iron-sulfur protein 3
NDUV1	Ubiquinone oxidoreductase core subunit V1
ALDOA	Aldolase A
MYOM1	Myomesin-1
PYGM	Myophosphorylase
RYR1	Ryanodine receptor 1
MYLPF	Myosin light chain, phosphorylatable, fast
MYH4	Myosin-4
MYH6	Myosin-6
MYH7b	Myosin7b
CYC	Cytochrome C
ENO1	Enolase 1
ULK1	Unc-51 Like Autophagy Activating Kinase 1
ATGs	Autophagy related proteins
RAB3	Ras related protein 3
NMJ	Neuromuscular junction
UPR	Unfolded protein response
PERK	Protein kinase R (PKR)-like endoplasmic reticulum kinase
IRE1α	Inositol-requiring protein 1α
ATF	Activating transcription factor
CHOP	C/EBP Homologous Protein
GADD34	Growth arrest and DNA damage-inducible protein
p53	Tumor protein 53
NF-κB	Nuclear factor kappa-light-chain-enhancer of activated B cells
Nrf2	Nuclear erythroid transcription factor 2
IL-6	Interleukine 6
TNFα	Tumor Necrosis Factorα
IL-1β	Interleukine 1β
Nqo1	NAD(P)H dehydrogenase (quinone 1)
Ho-1	Heme oxygenase-1
PFKP	Phosphofruktokinase

Supplementary Information

The online version contains supplementary material available at <https://doi.org/10.1186/s40478-025-01997-y>.

Supplementary Material 1
Supplementary Material 2
Supplementary Material 3
Supplementary Material 4

Author contributions

VR: performed animal experiments, Western-blot, analyzed data, wrote the paper; CFV: performed muscle histologic analysis and EM, discussed data and the design of the study, critically revised the paper; MS: discussed data and experimental plan, critically revised the paper; ADA: analyzed omics data, wrote the paper; MD and DS: performed omics and analyzed data; EF: carried out Western-blot and Ips, analyzed data; AH: collected clinical lab and clinical data of patients with VPS13A disease of the study, discussed data and critically revised the manuscript; LS: functional analyses; AS: performed animal experiments; IA: RT-PCR analyses, analyzed data and wrote the paper; SLA: discussed data and experimental plan, critically revised the paper; JC: data analyses, paper editing; Al: analyzed data and critically revised the paper; GV: carried out histologic analysis, wrote the paper; AD: critically revised the paper; RHW: critically revised the paper; AM, MO, MD, MA collected clinical lab and clinical data of patients with VPS13A disease of the study, performed muscle biopsies in healthy subjects and in patients with VPS13A disease; CB: performed muscle histologic analysis, analyzed data; KP: collected clinical lab and clinical data of patients with VPS13A disease of the study, discussed data and critically revised the manuscript; VS performed rotarod, behavior tests and analyzed data; PF revised and critically discussed data on rotarod and behavior tests; LDF: designed the study, analyzed and discussed data, and wrote the manuscript.

Funding

This paper was supported by the Advocacy for Neuroanthocytosis patients (LDF, RHW), FUR-UNIVR (LDF), Dept of Veterans Affairs (CX0002342, RHW). AH is supported by the Hermann und Lilly Schilling-Stiftung für medizinische

Forschung im Stifterverband. KP was supported by Rostock Academy of Science (RAS).

Data availability

No datasets were generated or analysed during the current study.

Declarations

Ethics approval and consent to participate

The Institutional Animal Experimental Committee of University of Verona (CIRSAL) and Italian Ministry of health approved the experimental protocol (56DC9.12) following European directive 2010/63/EU and the federation for laboratory animal science associations guidelines and recommendations. The muscle biopsies of patients with VPS13A disease were obtained for routine diagnostic reasons (P1 and P2) and postmortem (P3). Retrospective scientific use of remaining biopsy specimens/muscle samples was approved by the institutional review boards of the University Medical Center Rostock (A 2022-0058) and University Medicine Halle (2021 – 101).

Consent for publication

Not applicable.

Competing interests

The authors declare no competing interests.

Author details

¹Department of Engineering for Innovative Medicine- DIMI, University of Verona, Verona, Italy

²Department of Biomedical Sciences, University of Padua, Padua, Italy

³Venetian Institute of Molecular Medicine, Padova, Italy

⁴Department of Biochemistry and Molecular Genetics, University of Colorado School of Medicine, Aurora, CO, USA

⁵Translational Neurodegeneration Section "Albrecht Kossel", Department of Neurology, University Medical Center Rostock, University of Rostock, Rostock, Germany

⁶Center for Transdisciplinary Neurosciences Rostock (CTNR), University Medical Center Rostock, Rostock, Germany

⁷United Neuroscience Campus Lund-Rostock (UNC), Rostock site, Rostock, Germany

⁸Clinical Genetics Unit, Department of Women's and Children's Health, University of Padova, Padova, Italy

⁹Pediatric Research Institute (IRP) - Fondazione Città della Speranza, Padova, Italy

¹⁰Azienda Ospedaliera Universitaria Integrata Verona, Verona, Italy

¹¹Dipartimento di Medicina Molecolare e Biotecnologie Mediche, Università degli Studi di Napoli Federico II, Napoli, Italy

¹²CEINGE Biotecnologie Avanzate Franco Salvatore, Napoli, Italy

¹³Division of Nephrology, Beth Israel Deaconess Medical Center, Department of Medicine, Harvard Medical School, Boston, MA, USA

¹⁴Department of Neuroscience, Biomedicine and Movement Science, University of Verona, Verona, Italy

¹⁵Neurologische Klinik und Poliklinik, LMU Klinikum, LMU München, München, Germany

¹⁶Department of Neurology, James J. Peters Veterans Affairs Medical Center, Bronx, NY, USA

¹⁷Department of Neurology, Mount Sinai School of Medicine, New York City, NY, USA

¹⁸Department of Neurology, Martin-Luther-University of Halle-Wittenberg, Halle (Saale), Germany

¹⁹Department of Neurology, Klinikum Rechts der Isar, School of Medicine and Health, Technical University of Munich, München, Germany

²⁰Goethe University, University Hospital Frankfurt, Neurological Institute (Edinger Institute), Frankfurt am Main, Germany

²¹Goethe University, University Hospital Frankfurt, University Cancer Center (UCT) Frankfurt-Marburg, Frankfurt am Main, Germany

²²Goethe University, University Hospital Frankfurt, Frankfurt Cancer Institute (FCI), Frankfurt am Main, Germany

²³German Cancer Consortium (DKTK), Partner site Frankfurt / Mainz and German Cancer Research Center (DKFZ), Heidelberg, Germany

²⁴Mitochondria and Metabolism Imaging Core, Department of Endocrinology, University of California, Los Angeles, USA

²⁵Section of Anatomy and Histology, Department of Excellence in Neurosciences, Biomedicine and Movement Sciences, University of Verona, Verona, Italy

Received: 18 February 2025 / Accepted: 3 April 2025

Published online: 24 April 2025

References

- Afroze D, Kumar A (2019) ER stress in skeletal muscle remodeling and myopathies. *FEBS J* 286:379–398. <https://doi.org/10.1111/febs.14358>
- Ahn B, Pharaoh G, Premkumar P, Huseman K, Ranjit R, Kinter M, Szeweda L, Kiss T, Fulop G, Tarantini S, Csiszar A, Ungvari Z, Van Remmen H (2018) Nrf2 deficiency exacerbates age-related contractile dysfunction and loss of skeletal muscle mass. *Redox Biol* 17:47–58. <https://doi.org/10.1016/j.redox.2018.04.004>
- Braidly N, Berg J, Clement J, Khorshidi F, Poljak A, Jayasena T, Grant R, Sachdev P (2019) Role of nicotinamide adenine dinucleotide and related precursors as therapeutic targets for Age-Related degenerative diseases: rationale, biochemistry, pharmacokinetics, and outcomes. *Antioxid Redox Signal* 30:251–294. <https://doi.org/10.1089/ars.2017.7269>
- Buttgereit F, Brand MD (1995) A hierarchy of ATP-consuming processes in mammalian cells. *Biochem J* 312(Pt 1):163–167. <https://doi.org/10.1042/bj3120163>
- Cai D, Frantz JD, Tawa NE Jr., Melendez PA, Oh BC, Lidov HG, Hasselgren PO, Frontera WR, Lee J, Glass DJ, Shoelson SE (2004) IKKbeta/NF-kappaB activation causes severe muscle wasting in mice. *Cell* 119:285–298. <https://doi.org/10.1016/j.cell.2004.09.027>
- Carnio S, LoVerso F, Baraibar MA, Longa E, Khan MM, Maffei M, Reischl M, Canepari M, Loeffler S, Kern H, Blaauw B, Friguet B, Bottinelli R, Rudolf R, Sandri M (2014) Autophagy impairment in muscle induces neuromuscular junction degeneration and precocious aging. *Cell Rep* 8:1509–1521. <https://doi.org/10.1016/j.celrep.2014.07.061>
- Casas-Martinez JC, Samali A, McDonagh B (2024) Redox regulation of UPR signalling and mitochondrial ER contact sites. *Cell Mol Life Sci* 81:250. <https://doi.org/10.1007/s00018-024-05286-0>
- Chabi B, Ljubivic V, Menzies KJ, Huang JH, Saleem A, Hood DA (2008) Mitochondrial function and apoptotic susceptibility in aging skeletal muscle. *Aging Cell* 7:2–12. <https://doi.org/10.1111/j.1474-9726.2007.00347.x>
- Chen M, Wang Y, Deng S, Lian Z, Yu K (2022) Skeletal muscle oxidative stress and inflammation in aging: focus on antioxidant and anti-inflammatory therapy. *Front Cell Dev Biol* 10:964130. <https://doi.org/10.3389/fcell.2022.964130>
- Chicco AJ, Le CH, Gnaiger E, Dreyer HC, Muyskens JB, D'Alessandro A, Nemkov T, Hocker AD, Prenni JE, Wolfe LM, Sindt NM, Lovering AT, Subudhi AW, Roach RC (2018) Adaptive remodeling of skeletal muscle energy metabolism in high-altitude hypoxia: lessons from altitudinomics. *J Biol Chem* 293:6659–6671. <https://doi.org/10.1074/jbc.RA117.000470>
- Covarrubias AJ, Perrone R, Grozio A, Verdin E (2021) NAD(+) metabolism and its roles in cellular processes during ageing. *Nat Rev Mol Cell Biol* 22:119–141. <https://doi.org/10.1038/s41580-020-00313-x>
- D'Alessandro A, Hay A, Dzieciatkowska M, Brown BC, Morrison EJ, Hansen KC, Zimring JC (2021) Protein-L-isoaspartate O-methyltransferase is required for in vivo control of oxidative damage in red blood cells. *Haematologica* 106:2726–2739. <https://doi.org/10.3324/haematol.2020.266676>
- D'Alessandro A, Keele GR, Hay AM, Nemkov T, Earley EJ, Stephenson D, Vincent M, Deng X, Stone M, Dzieciatkowska M, Hansen KC, Kleinman SH, Spitalnik SL, Roubinian NH, Norris PJ, Busch MP, Page GP, Stockwell B, Churchill GA, Zimring JC (2024) Ferroptosis regulates hemolysis in stored murine and human red blood cells. *Blood*. <https://doi.org/10.1182/blood.2024026109>
- De Franceschi L, Brugnara C, Beuzard Y (1997) Dietary magnesium supplementation ameliorates anemia in a mouse model of beta-thalassemia. *Blood* 90:1283–1290
- Dias C, Nylandsted J (2021) Plasma membrane integrity in health and disease: significance and therapeutic potential. *Cell Discov* 7:4. <https://doi.org/10.1038/s41421-020-00233-2>
- Egan DF, Shackelford DB, Mihaylova MM, Gelino S, Kohnz RA, Mair W, Vasquez DS, Joshi A, Gwinn DM, Taylor R, Asara JM, Fitzpatrick J, Dillin A, Viollet B, Kundu M, Hansen M, Shaw RJ (2011) Phosphorylation of ULK1 (hATG1) by AMP-activated protein kinase connects energy sensing to mitophagy. *Science* 331:456–461. <https://doi.org/10.1126/science.1196371>
- Erekat N, Al-Jarrah MD (2018) Interleukin-1 beta and tumor necrosis factor alpha upregulation and nuclear factor kappa B activation in skeletal muscle from a mouse model of chronic/progressive Parkinson disease. *Med Sci Monit* 24:7524–7531. <https://doi.org/10.12659/MSM.909032>
- Estebanez B, de Paz JA, Cuevas MJ, Gonzalez-Gallego J (2018) Endoplasmic reticulum unfolded protein response, aging and exercise: an update. *Front Physiol* 9:1744. <https://doi.org/10.3389/fphys.2018.01744>
- Fiacco E, Castagnetti F, Bianconi V, Madaro L, De Bardi M, Nazio F, D'Amico A, Bertini E, Cecconi F, Puri PL, Latella L (2016) Autophagy regulates satellite cell ability to regenerate normal and dystrophic muscles. *Cell Death Differ* 23:1839–1849. <https://doi.org/10.1038/cdd.2016.70>
- Franceschi C, Capri M, Monti D, Giunta S, Olivieri F, Sevini F, Panourgia MP, Invidia L, Celani L, Scurti M, Cevenini E, Castellani GC, Salvioli S (2007) Inflammaging and anti-inflammaging: a systemic perspective on aging and longevity emerged from studies in humans. *Mech Ageing Dev* 128:92–105. <https://doi.org/10.1016/j.mad.2006.11.016>
- Fu P, Gong L, Yang L, Tang S, Ma F (2023) Weight bearing training alleviates muscle atrophy and pyroptosis of middle-aged rats. *Front Endocrinol (Lausanne)* 14:1202686. <https://doi.org/10.3389/fendo.2023.1202686>
- Gao Y, Kim K, Vitrac H, Salazar RL, Gould BD, Soedkamp D, Spivia W, Raedschelders K, Dinh AQ, Guzman AG, Tan L, Azinas S, Taylor DJR, Schiffer W, McNavish D, Burks HB, Gottlieb RA, Lorenzi PL, Hanson BM, Van Eyk JE, Taegtmeier H, Karlstaedt A (2024) Autophagic signaling promotes systems-wide remodeling in skeletal muscle upon Oncometabolic stress by D2-HG. *Mol Metab* 86:101969. <https://doi.org/10.1016/j.molmet.2024.101969>
- Garcia-Garcia VA, Alameda JP, Page A, Casanova ML (2021) Role of NF-kappaB in ageing and Age-Related diseases: lessons from genetically modified mouse models. *Cells* 10. <https://doi.org/10.3390/cells10081906>
- Garrick JM, Costa LG, Cole TB, Marsillach J (2021) Evaluating gait and locomotion in rodents with the catwalk. *Curr Protoc* 1:e220. <https://doi.org/10.1002/cpz1.220>
- Guntur VP, Nemkov T, de Boer E, Mohning MP, Baraghoshi D, Cendali FI, San-Millan I, Petrache I, D'Alessandro A (2022) Signatures of Mitochondrial Dysfunction and Impaired Fatty Acid Metabolism in Plasma of Patients with Post-Acute Sequelae of COVID-19 (PASC). *Metabolites* 12. <https://doi.org/10.3390/metabo12111026>
- Han YH, Jin MH, Jin YH, Yu NN, Liu J, Zhang YQ, Cui YD, Wang AG, Lee DS, Kim SU, Kim JS, Kwon T, Sun HN (2020) Deletion of Peroxiredoxin II inhibits the growth of mouse primary mesenchymal stem cells through induction of the G(0)/G(1) Cell-cycle arrest and activation of AKT/GSK3β/β-Catenin signaling. *Vivo* 34:133–141. <https://doi.org/10.21873/invivo.11754>
- Hanna M, Guillen-Samander A, De Camilli P (2023) RBG motif Bridge-Like lipid transport proteins: structure, functions, and open questions. *Annu Rev Cell Dev Biol* 39:409–434. <https://doi.org/10.1146/annurev-cellbio-120420-014634>
- Hetz C (2012) The unfolded protein response: controlling cell fate decisions under ER stress and beyond. *Nat Rev Mol Cell Biol* 13:89–102. <https://doi.org/10.1038/nrm3270>
- Ishikawa S, Tachibana N, Tabata KI, Fujimori N, Hayashi RI, Takahashi J, Ikeda SI, Hanyu N (2000) Muscle CT scan findings in McLeod syndrome and chorea-acanthocytosis. *Muscle Nerve* 23:1113–1116. [https://doi.org/10.1002/1097-4598\(200007\)23:7%3C1113::aid-mus15%3E3.0.co;2-6](https://doi.org/10.1002/1097-4598(200007)23:7%3C1113::aid-mus15%3E3.0.co;2-6)
- Jezeq P, Jaburek M, Holendova B, Engstova H, Dlaskova A (2023) Mitochondrial Cristae morphology reflecting metabolism, superoxide formation, redox homeostasis, and pathology. *Antioxid Redox Signal* 39:635–683. <https://doi.org/10.1089/ars.2022.0173>
- Ji Y, Jiang Q, Chen B, Chen X, Li A, Shen D, Shen Y, Liu H, Qian X, Yao X, Sun H (2025) Endoplasmic reticulum stress and unfolded protein response: roles in skeletal muscle atrophy. *Biochem Pharmacol* 234:116799. <https://doi.org/10.1016/j.bcp.2025.116799>
- Ju JS, Varadhachary AS, Miller SE, Weihl CC (2010) Quantitation of autophagic flux in mature skeletal muscle. *Autophagy* 6:929–935. <https://doi.org/10.4161/auto.6.7.12785>
- Kawakami Y, Hambright WS, Takayama K, Mu X, Lu A, Cummins JH, Matsu-moto T, Yurube T, Kuroda R, Kurosaka M, Fu FH, Robbins PD, Niedernhofer LJ, Huard J (2019) Rapamycin rescues Age-Related changes in Muscle-Derived stem/progenitor cells from progeroid mice. *Mol Ther Methods Clin Dev* 14:64–76. <https://doi.org/10.1016/j.omtm.2019.05.011>
- Krishna S, Spaulding HR, Koltes JE, Quindry JC, Valentine RJ, Selsby JT (2023) Indicators of increased ER stress and UPR in aged D2-mdx and human dystrophic skeletal muscles. *Front Physiol* 14:1152576. <https://doi.org/10.3389/fphys.2023.1152576>

35. Leduc-Gaudet JP, Franco-Romero A, Cefis M, Moamer A, Broering FE, Milan G, Sartori R, Chaffer TJ, Dulac M, Marcangeli V, Mayaki D, Huck L, Shams A, Morais JA, Duchesne E, Lochmuller H, Sandri M, Hussain SNA, Gousspillou G (2023) MYTHO is a novel regulator of skeletal muscle autophagy and integrity. *Nat Commun* 14:1199. <https://doi.org/10.1038/s41467-023-36817-1>
36. Li Y, Guo Y, Tang J, Jiang J, Chen Z (2014) New insights into the roles of CHOP-induced apoptosis in ER stress. *Acta Biochim Biophys Sin* (Shanghai) 46:629–640. <https://doi.org/10.1093/abbs/gmu048>
37. Limos LC, Ohnishi A, Sakai T, Fujii N, Goto I, Kuroiwa Y (1982) Myopathic changes in chorea-acanthocytosis. Clinical and histopathological studies. *J Neurol Sci* 55:49–58. [https://doi.org/10.1016/0022-510x\(82\)90169-1](https://doi.org/10.1016/0022-510x(82)90169-1)
38. Lupo F, Tibaldi E, Matte A, Sharma AK, Brunati AM, Alper SL, Zancanaro C, Benati D, Siciliano A, Bertoldi M, Zonta F, Storch A, Walker RH, Danek A, Bader B, Hermann A, De Franceschi L (2016) A new molecular link between defective autophagy and erythroid abnormalities in chorea-acanthocytosis. *Blood* 128:2976–2987. <https://doi.org/10.1182/blood-2016-07-727321>
39. Maccarinelli F, Pagani A, Cozzi A, Codazzi F, Di Giacomo G, Capoccia S, Rapino S, Finazzi D, Politi LS, Cirulli F, Giorgio M, Cremona O, Grohovaz F, Levi S (2015) A novel neuroferritinopathy mouse model (FTL 498InsTC) shows progressive brain iron dysregulation, morphological signs of early neurodegeneration and motor coordination deficits. *Neurobiol Dis* 81:119–133. <https://doi.org/10.1016/j.nbd.2014.10.023>
40. Makrecka-Kuka M, Sevostjanovs E, Vilks K, Volska K, Antone U, Kuka J, Makarova E, Pugovics O, Dambrova M, Liepinsh E (2017) Plasma acylcarnitine concentrations reflect the acylcarnitine profile in cardiac tissues. *Sci Rep* 7:17528. <https://doi.org/10.1038/s41598-017-17797-x>
41. Mammucari C, Milan G, Romanello V, Masiero E, Rudolf R, Del Piccolo P, Burden SJ, Di Lisi R, Sandri C, Zhao J, Goldberg AL, Schiaffino S, Sandri M (2007) FoxO3 controls autophagy in skeletal muscle in vivo. *Cell Metab* 6:458–471. <https://doi.org/10.1016/j.cmet.2007.11.001>
42. Matte A, Low PS, Turrini F, Bertoldi M, Campanella ME, Spano D, Pantaleo A, Siciliano A, De Franceschi L (2010) Peroxiredoxin-2 expression is increased in beta-thalassemic mouse red cells but is displaced from the membrane as a marker of oxidative stress. *Free Radic Biol Med* 49:457–466. <https://doi.org/10.1016/j.freeradbiomed.2010.05.003>
43. Matte A, Federti E, Kung C, Kosinski PA, Narayanaswamy R, Russo R, Federico G, Carlomagno F, Desbats MA, Salviati L, Leboeuf C, Valenti MT, Turrini F, Janin A, Yu S, Beneduce E, Ronseaux S, Iatcenko I, Dang L, Ganz T, Jung CL, Iolascon A, Brugnara C, De Franceschi L (2021) The pyruvate kinase activator mitapivat reduces hemolysis and improves anemia in a beta-thalassemia mouse model. *J Clin Invest* 131. <https://doi.org/10.1172/JCI144206>
44. Melone MA, Di Fede G, Peluso G, Lus G, Di Iorio G, Sampaolo S, Capasso A, Gentile V, Cotrufo R (2002) Abnormal accumulation of TtGase products in muscle and erythrocytes of chorea-acanthocytosis patients. *J Neuropathol Exp Neurol* 61:841–848. <https://doi.org/10.1093/jnen/61.10.841>
45. Migliavacca E, Tay SKH, Patel HP, Sonntag T, Civiletto G, McFarlane C, Forrester T, Barton SJ, Leow MK, Antoun E, Charpagne A, Seng Chong Y, Descombes P, Feng L, Francis-Emmanuel P, Garratt ES, Giner MP, Green CO, Karaz S, Kothandaraman N, Marquis J, Metairon S, Moco S, Nelson G, Ngo S, Pleasants T, Raymond F, Sayer AA, Ming Sim C, Slater-Jefferies J, Syddall HE, Fang Tan P, Titcombe P, Vaz C, Westbury LD, Wong G, Yonghui W, Cooper C, Sheppard A, Godfrey KM, Lillycrop KA, Karnani N, Feige JN (2019) Mitochondrial oxidative capacity and NAD(+) biosynthesis are reduced in human sarcopenia across ethnicities. *Nat Commun* 10:5808. <https://doi.org/10.1038/s41467-019-1369-4-1>
46. Milan G, Romanello V, Pescatore F, Armani A, Paik JH, Frasson L, Seydel A, Zhao J, Abraham R, Goldberg AL, Blaauw B, DePinho RA, Sandri M (2015) Regulation of autophagy and the ubiquitin-proteasome system by the FoxO transcriptional network during muscle atrophy. *Nat Commun* 6:6670. <https://doi.org/10.1038/ncomms7670>
47. Miller CJ, Gounder SS, Kannan S, Goutam K, Muthusamy VR, Firpo MA, Symons JD, Paine R 3rd, Hoidal JR, Rajasekaran NS (2012) Disruption of Nrf2/ARE signaling impairs antioxidant mechanisms and promotes cell degradation pathways in aged skeletal muscle. *Biochim Biophys Acta* 1822:1038–1050. <https://doi.org/10.1016/j.bbadis.2012.02.007>
48. Nemkov T, Reisz JA, Gehrke S, Hansen KC, D'Alessandro A (2019) High-Throughput metabolomics: isocratic and gradient mass Spectrometry-Based methods. *Methods Mol Biol* 1978:13–26. https://doi.org/10.1007/978-1-4939-9236-2_2
49. Nemkov T, Stephenson D, Earley EJ, Keele GR, Hay A, Key A, Haiman ZB, Erickson C, Dzieciatkowska M, Reisz JA, Moore A, Stone M, Deng X, Kleinman S, Spitalnik SL, Hod EA, Hudson KE, Hansen KC, Palsson BO, Churchill GA, Roubinian N, Norris PJ, Busch MP, Zimring JC, Page GP, D'Alessandro A (2024) Biological and genetic determinants of glycolysis: phosphofructokinase isoforms boost energy status of stored red blood cells and transfusion outcomes. *Cell Metab* 36(1979–1997 e1913). <https://doi.org/10.1016/j.cmet.2024.06.007>
50. Oyadomari S, Mori M (2004) Roles of CHOP/GADD153 in Endoplasmic reticulum stress. *Cell Death Differ* 11:381–389. <https://doi.org/10.1038/sj.cdd.4401373>
51. Parker E, Khayrullin A, Kent A, Mendhe B, Youssef El Baradie KB, Yu K, Pihkala J, Liu Y, McGee-Lawrence M, Johnson M, Chen J, Hamrick M (2021) Hindlimb immobilization increases IL-1beta and Cdkn2a expression in skeletal muscle Fibro-Adipogenic progenitor cells: A link between senescence and muscle disuse atrophy. *Front Cell Dev Biol* 9:790437. <https://doi.org/10.3389/fcell.2021.790437>
52. Peikert K, Danek A, Hermann A (2018) Current state of knowledge in Choreo-Acanthocytosis as core neuroacanthocytosis syndrome. *Eur J Med Genet* 61:699–705. <https://doi.org/10.1016/j.ejmg.2017.12.007>
53. Peikert K, Federti E, Matte A, Constantino G, Pietronigro EC, Fabene PF, Defilippi P, Turco E, Del Gallo F, Pucci P, Amoresano A, Illiano A, Cozzolino F, Monti M, Garelli F, Terreno E, Alper SL, Glass H, Pelz L, Akgun K, Ziemssen T, Ordemann R, Lang F, Brunati AM, Tibaldi E, Andolfo I, Iolascon A, Bertini G, Buffelli M, Zancanaro C, Lorenzetto E, Siciliano A, Bonifacio M, Danek A, Walker RH, Hermann A, De Franceschi L (2021) Therapeutic targeting of Lyn kinase to treat chorea-acanthocytosis. *Acta Neuropathol Commun* 9:81. <https://doi.org/10.1186/s40478-021-01181-y>
54. Peikert K, Rampoldi CD-SL, Miltenberger-Miltenyi G, Neiman A, De Camilli P, Hermann A, Walker RH, Monaco AP, Danek A (2023) VPS13ADisease. Gene reviews. University of Washington, Seattle (WA), USA, Seattle (WA), USA
55. Reid MB, Li YP (2001) Tumor necrosis factor-alpha and muscle wasting: a cellular perspective. *Respir Res* 2:269–272. <https://doi.org/10.1186/rr67>
56. Rinaldo P, Cowan TM, Matern D (2008) Acylcarnitine profile analysis. *Genet Med* 10:151–156. <https://doi.org/10.1097/GIM.0b013e3181614289>
57. Safdar A, deBeer J, Tarnopolsky MA (2010) Dysfunction of Nrf2-Keap1 redox signaling in skeletal muscle of the sedentary old. *Free Radic Biol Med* 49:1487–1493. <https://doi.org/10.1016/j.freeradbiomed.2010.08.010>
58. Saiki S, Sakai K, Murata KY, Saiki M, Nakanishi M, Kitagawa Y, Kaito M, Gondo Y, Kumamoto T, Matsui M, Hattori N, Hirose G (2007) Primary skeletal muscle involvement in chorea-acanthocytosis. *Mov Disord* 22:848–852. <https://doi.org/10.1002/mds.21437>
59. Santoro A, Martucci M, Conte M, Capri M, Franceschi C, Salvioli S (2020) Inflammaging, hormesis and the rationale for anti-aging strategies. *Ageing Res Rev* 64:101142. <https://doi.org/10.1016/j.arr.2020.101142>
60. Sartori R, Romanello V, Sandri M (2021) Mechanisms of muscle atrophy and hypertrophy: implications in health and disease. *Nat Commun* 12:330. <https://doi.org/10.1038/s41467-020-20123-1>
61. Senft D, Ronai ZA (2015) UPR, autophagy, and mitochondria crosstalk underlies the ER stress response. *Trends Biochem Sci* 40:141–148. <https://doi.org/10.1016/j.tibs.2015.01.002>
62. Stanslowsky N, Reinhardt P, Glass H, Kalmbach N, Naujock M, Hensel N, Lubben V, Pal A, Venneri A, Lupo F, De Franceschi L, Claus P, Sternecker J, Storch A, Hermann A, Wegner F (2016) Neuronal dysfunction in iPSC-Derived medium spiny neurons from Choreo-Acanthocytosis patients is reversed by Src kinase Inhibition and F-Actin stabilization. *J Neurosci* 36:12027–12043. <https://doi.org/10.1523/JNEUROSCI.0456-16.2016>
63. Tam NN, Chung SS, Lee DT, Wong YC (2000) Aberrant expression of hepatocyte growth factor and its receptor, c-Met, during sex hormone-induced prostatic carcinogenesis in the noble rat. *Carcinogenesis* 21:2183–2191. <https://doi.org/10.1093/carcin/21.12.2183>
64. Tamura Y, Matsui K, Yaguchi H, Hashimoto M, Inoue K (2005) Nemaline rods in chorea-acanthocytosis. *Muscle Nerve* 31:516–519. <https://doi.org/10.1002/mus.20243>
65. Tilstra JS, Robinson AR, Wang J, Gregg SQ, Clauson CL, Reay DP, Nasto LA, St Croix CM, Usas A, Vo N, Huard J, Clemens PR, Stolz DB, Guttridge DC, Watkins SC, Garinis GA, Wang Y, Niedernhofer LJ, Robbins PD (2012) NF-kappaB Inhibition delays DNA damage-induced senescence and aging in mice. *J Clin Invest* 122:2601–2612. <https://doi.org/10.1172/JCI45785>
66. Tomemori Y, Ichiba M, Kusumoto A, Mizuno E, Sato D, Muroya S, Nakamura M, Kawaguchi H, Yoshida H, Ueno S, Nakao K, Nakamura K, Aiba A, Katsuki M, Sano A (2005) A gene-targeted mouse model for chorea-acanthocytosis. *J Neurochem* 92:759–766. <https://doi.org/10.1111/j.1471-4159.2004.02924.x>
67. Vaisfeld A, Bruno G, Petracca M, Bentivoglio AR, Servidei S, Vita MG, Bove F, Straccia G, Dato C, Di Iorio G, Sampaolo S, Peluso S, De Rosa A, De Michele G,

- Barghigiani M, Galatolo D, Tessa A, Santorelli F, Chiurazzi P, Melone MAB (2021) Neuroacanthocytosis syndromes in an Italian cohort: clinical spectrum, high genetic variability and muscle involvement. *Genes (Basel)* 12. <https://doi.org/10.3390/genes12030344>
68. Vasilaki A, van der Meulen JH, Larkin L, Harrison DC, Pearson T, Van Remmen H, Richardson A, Brooks SV, Jackson MJ, McArdle A (2010) The age-related failure of adaptive responses to contractile activity in skeletal muscle is mimicked in young mice by deletion of Cu,Zn superoxide dismutase. *Aging Cell* 9:979–990. <https://doi.org/10.1111/j.1474-9726.2010.00635.x>
69. Vasilaki A, Pollock N, Giakoumaki I, Goljanek-Whysall K, Sakellariou GK, Pearson T, Kayani A, Jackson MJ, McArdle A (2016) The effect of lengthening contractions on neuromuscular junction structure in adult and old mice. *Age (Dordr)* 38:259–272. <https://doi.org/10.1007/s11357-016-9937-7>
70. Walker RH, Danek A (2021) Neuroacanthocytosis - Overdue for a taxonomic update. *Tremor Other Hyperkinet Mov (N Y)* 11:1. <https://doi.org/10.5334/tohm.583>
71. Wang C, Wang H, Zhang D, Luo W, Liu R, Xu D, Diao L, Liao L, Liu Z (2018) Phosphorylation of ULK1 affects autophagosome fusion and links chaperone-mediated autophagy to macroautophagy. *Nat Commun* 9:3492. <https://doi.org/10.1038/s41467-018-05449-1>
72. Zhang X, Habiballa L, Aversa Z, Ng YE, Sakamoto AE, Englund DA, Pearsall VM, White TA, Robinson MM, Rivas DA, Dasari S, Hraby AJ, Lagnado AB, Jachim SK, Granic A, Sayer AA, Jurk D, Lanza IR, Khosla S, Fielding RA, Nair KS, Schafer MJ, Passos JF, LeBrasseur NK (2022) Characterization of cellular senescence in aging skeletal muscle. *Nat Aging* 2:601–615. <https://doi.org/10.1038/s43587-022-00250-8>

Publisher's note

Springer Nature remains neutral with regard to jurisdictional claims in published maps and institutional affiliations.